

Fluctuations and distributions in random aggregates

Paul Meakin

*Central Research and Development Department, E.I. du Pont de Nemours and Company,
Experimental Station, Wilmington, Delaware 19898*

Shlomo Havlin

Department of Physics, Bar-Ilan University, 52 100 Ramat-Gan, Israel

(Received 28 May 1987)

We have measured the distribution of mass $P_s(r)$ within a distance r measured from occupied sites in the screened-growth model ($d_f = 1.25, 1.5$, and 1.75 , where d_f is the fractal dimension), off-lattice diffusion-limited cluster-cluster aggregates ($d_f = 1.43$), and off-lattice diffusion-limited aggregation (DLA) clusters. Here $P_s(r)$ is the probability that a circle of radius r centered on an occupied site will contain S occupied sites or particles. For the screened-growth and cluster-cluster aggregation models, the distributions $P_s(r)$ can be described in terms of the scaling form $P_s(r) \sim S^{-1} f(S/r^{d_f})$. The dependence of the moments $\langle S^n \rangle / \langle S \rangle^n$ on the distance r has also been measured. For the screened-growth and cluster-cluster aggregation models these quantities are essentially independent of r for $n \geq 1$. For DLA the simple scaling form for $P_s(r)$ does not describe the mass distribution and $(1/n) \ln(\langle S^n \rangle / \langle S \rangle^n)$, with $n = 2-10$, has a linear dependence on $\ln(r)$ with negative slopes which are different for different values of n for small values of r . Since $\langle S^n \rangle / \langle S \rangle^n$ has a lower bound of 1, this cannot be the true asymptotic behavior for off-lattice DLA. It suggests that DLA has a more complex structure than either the screened-growth model or cluster-cluster aggregation.

The structural properties of random aggregates have recently been the subject of considerable study.¹⁻⁷ It is well known that an aggregate cannot be fully characterized only by its fractal dimension.⁸ Much effort has been expended on the question of how to characterize fully the structural properties of random aggregates. It has recently been suggested by Meakin *et al.*⁹ and by Halsey *et al.*¹⁰ that the surface of diffusion-limited aggregation (DLA) requires an infinite hierarchy of fractal dimensions for its characterization. Similar hierarchies have been found in a variety of other areas of physics.¹¹⁻¹⁸

In this work we study the probability distribution $P_s(r)$ and the moments $\langle S^n \rangle$ of the mass S within a given radius r measured from randomly selected occupied sites on several types of random aggregates. The exponent d_f characterizing the first moment $\langle S \rangle \sim r^{d_f}$ is the fractal dimension of the aggregate. We carried out simulations of two-dimensional (2D) off-lattice DLA, 2D hierarchical diffusion-limited cluster-cluster aggregation (CCA), and screened-growth clusters (SGC) with fractal dimensionalities of 1.25, 1.5, and 1.75. We find that $P_s(r)$ for CCA and SGC behave quite differently from $P_s(r)$ of DLA. Whereas in CCA and SGC we find a scaling form for $P_s(r)$ and gap exponents for the moments, the data for DLA do not scale properly and a hierarchical set of effective exponents seems to describe the various moments.

Given a large random cluster, we chose randomly a site on the cluster. The quantity $P_s(r)$ is defined as the probability density that within a distance r of the chosen site there exists S sites of the cluster. The fractal dimen-

sion d_f is defined through the relation

$$\langle S \rangle = \int_0^\infty S P_s(r) dS \sim r^{d_f}. \quad (1)$$

The simplest scaling form for $P_s(r)$ that yields Eq. (1) is

$$P_s(r) \sim S^{-1} f(S/r^{d_f}). \quad (2)$$

The factor S^{-1} comes from the normalization condition of $P_s(r)$, i.e.,

$$\int_0^\infty P_s(r) dS = 1. \quad (3)$$

If Eq. (2) is valid, the moments can be easily calculated,

$$\langle S^n \rangle \sim \int_0^\infty S^n S^{-1} f(S/r^{d_f}) dS \sim r^{nd_f}, \quad n > 0, \quad (4)$$

and d_f is the gap exponent characterizing all of the positive moments of the mass.

The simple scaling theory given in Eqs. (2)–(4) was tested numerically on CCA, SGC, and DLA clusters. We first generated a large-size cluster (10 000–50 000 particles or occupied lattice sites). A large number of sites (typically 5000) on each cluster was selected randomly and we calculated the number of particles contained within a distance r from the selected sites. Using a large number of clusters, the quantity $N_s(r)$ was obtained. Here $N_s(r)$ is the number of circles of radius r which contain S particles. By dividing $N_s(r)$ by the total number of circles of size r , $P_s(r)$ is obtained.

For the screened-growth model^{19,20} the growth probability in unoccupied surface sites is given by

$$P_i \propto \prod_{j=1}^M \exp[-(A/r_{ij}^\epsilon)], \quad (5)$$

where r_{ij} is the distance from the i th unoccupied surface site to the j th occupied site in the growing cluster which contains M sites. It has been shown by computer simulations²⁰ and theoretically^{21,22} that this model leads to the formation of clusters with a fractal dimension d_f given by $d_f = \epsilon$, where ϵ is the exponent in the screening function. Figures 1–3 show the results for $N_s(r)$ obtained from 19 screened-growth clusters of 10 000 sites with a fractal dimensionality 1.5, 92 clusters of 6000 sites with a fractal dimensionality of 1.25, and 17 clusters of 15 000 sites with a fractal dimensionality of 1.75, respectively. For these models, and DLA, the randomly selected “origins” were picked from sites in the interior of the clusters and not too close to the growth sites. The origins were selected from those sites which were added when the growth process was between 10 and 50% complete. The results shown in Figs. 1(a), 2(a), and 3(a) support the factor S^{-1} in Eq. (2). Figures 1(b), 2(b), and 3(b) strongly support the scaling form of Eq. (2). Figures 1(b), 2(b), and 3(b) do show deviations from this scaling form which we attribute mainly to the fact that for small values of r we are not completely in the scaling regime. This is particularly evident in Fig. 2(b) where the curve for $r=5$ is pointed out.

Clusters generated using two-dimensional diffusion-limited cluster-cluster aggregation models^{23,24} have a fractal dimension of about 1.43. Here we used clusters

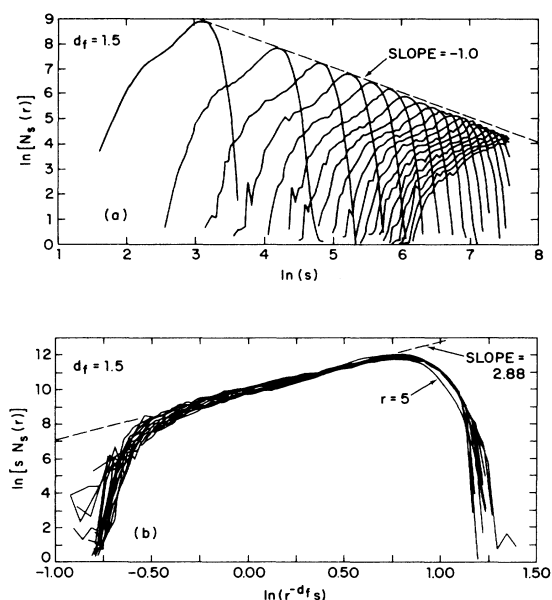


FIG. 1. The number of circles of radius r (centered on randomly selected occupied sites) which contain S occupied sites for screened-growth clusters which have a fractal dimension (d_f) of 1.5. Each curve corresponds to a different value of r ($r=5n$, $n=1-20$). (a) shows the distribution functions $N_s(r)$ and (b) shows how these curves can be scaled onto a common curve. (b) shows reasonably good data collapse, particularly for radii greater than five lattice units.

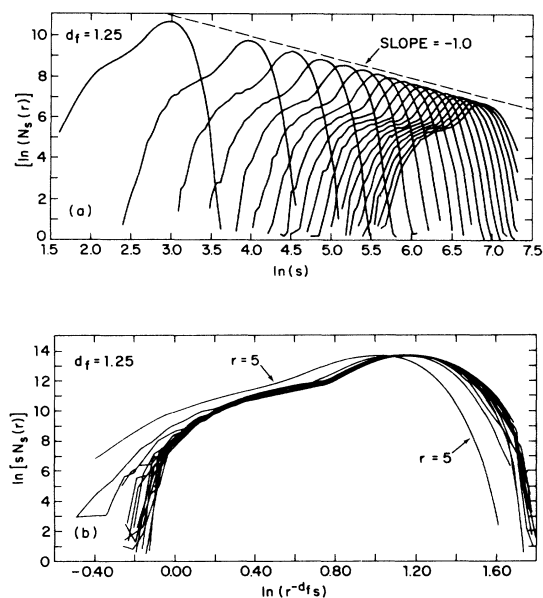


FIG. 2. The dependence of $\ln[N_s(r)]$ on $\ln(S)$ for screened-growth clusters with a fractal dimension of 1.25. Each curve corresponds to a different value of r ($r=5, 10, \dots, 100$). (b) shows how these curves can be scaled onto a common curve. The scaling works well except for small values of r .

generated using an off-lattice hierarchical²⁵ model described previously.²⁶ In this case the origins were selected randomly without any restrictions. Thirty 2^{14} (16 384) particle aggregates were generated and 5000 ori-

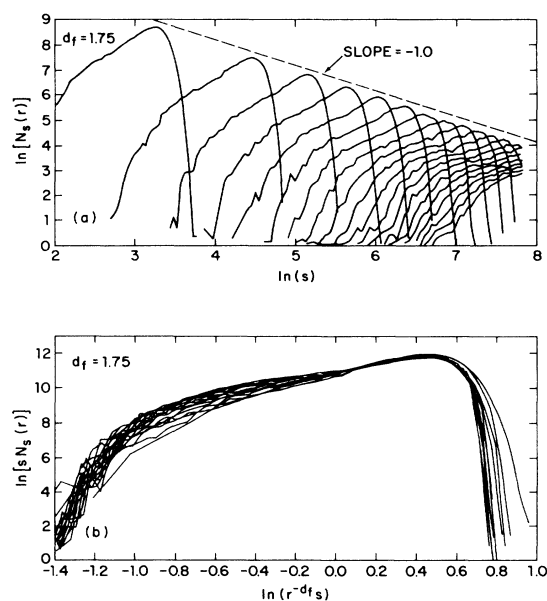


FIG. 3. This figure shows the results from simulations similar to those used to obtain the results displayed in Figs. 1 and 2. In this case an exponent (ϵ) of 1.75 was used in the screening function for the screened-growth model leading to structures with a fractal dimensionality of 1.75.

gins were selected on each cluster. The results from these simulations, which are shown in Fig. 4, also support the scaling form given in Eq. (2). Note that the only parameter needed for Eq. (2) is d_f which is found to be in agreement with the known values $d_f = 1.25, 1.5, 1.75$ for SGC and $d_f = 1.43$ for CCA. The shapes of the scaling functions $[f(x)]$ shown in Figs. 1(b), 2(b), 3(b), and 4(b) are all very similar. They are characterized by three regimes. Small values of S/r^{d_f} ($=x$) for which the scaling function $f(x)$ seems to increase exponentially. An intermediate regime, in which the scaling function exhibits power-law behavior, and a third regime (large values of S/r^{d_f}), for which an exponential decrease in $f(x)$ with increasing x is observed. The cutoff in $f(x)$ at large and small x is a consequence of the fact that $S_{\min} \sim S_{\max} \sim r^{d_f}$, where S_{\min} and S_{\max} are the maximum and minimum values for S .

In Figs. 5(a) and 6 we present results for the moments $\langle S^n \rangle / \langle S \rangle^n$ as a function of r . As seen from the figures, the quantity $\langle S^n \rangle / \langle S \rangle^n$ is essentially independent of r for the screened-growth clusters with $d_f = 1.5$ and for 2D CCA ($d_f = 1.43$). These results also support the scaling theory Eqs. (2)–(4) since $\langle S^n \rangle / \langle S \rangle^n$, according to Eq. (4), is independent of r . For the screened-growth clusters, simulations were also carried out in which (400 lattice unit) \times (400 lattice unit) areas at the center of each cluster were covered by grids with sides of length l , and the number of occupied grid elements with sides of length l containing S occupied lattice sites $[N_s(l)]$ was measured and used to obtain the distribution $P'_s(l)$. We find that this distribution can be described in terms of the scaling form

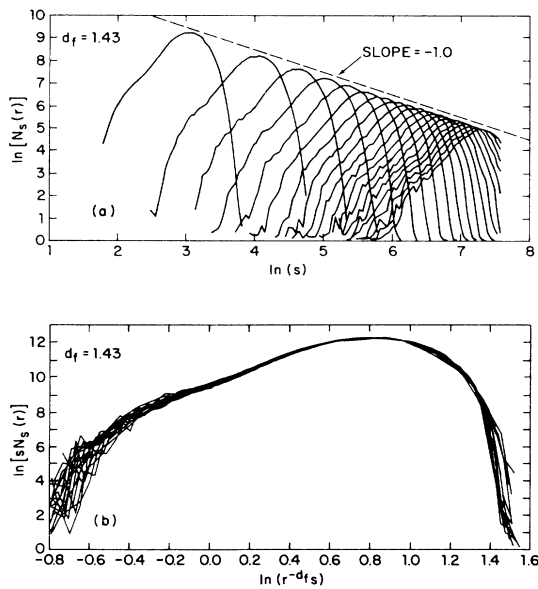


FIG. 4. The dependence of $\ln[N_s(r)]$ on $\ln(S)$ for 2D cluster-cluster aggregates generated using a 2D diffusion-limited off-lattice hierarchical model. Here the radii have values of $5n$ ($n = 1-20$) particle diameters. (b) illustrates the successful data collapse using the scaling form given in Eq. (2).

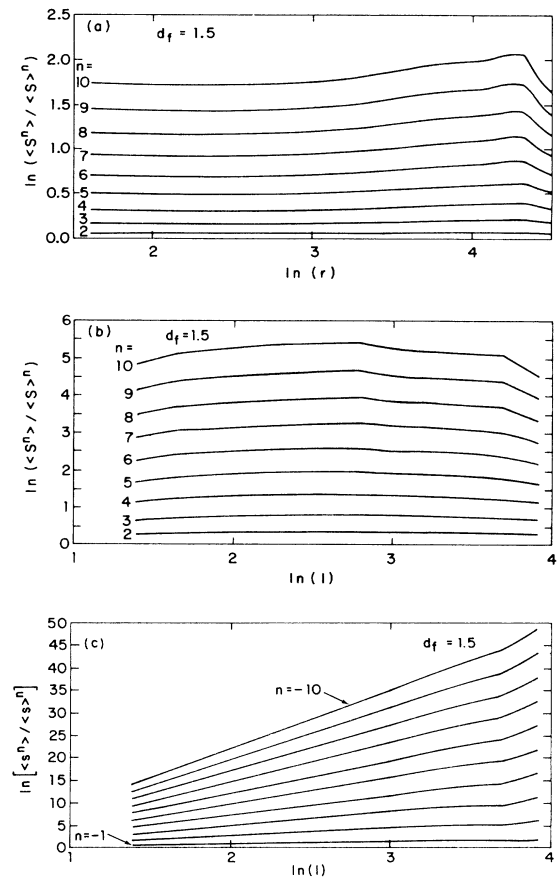


FIG. 5. (a) shows the dependence of $\ln(\langle S^n \rangle / \langle S \rangle^n)$ as a function of r for screened-growth clusters with a fractal dimension of 1.5. (b) shows similar results except that instead of measuring the number of occupied sites within a distance r from other occupied sites, a central region in each of the clusters was covered by grids with grid elements having sides of length l lattice units, and the number of occupied sites in each occupied grid element was used to determine $\langle S \rangle^n$ and $\langle S^n \rangle$. (c) shows the negative moments as a function of the grid element size (l). The mean number of occupied sites in an area of size l [$\langle S(l) \rangle$] was obtained by averaging over only those areas containing one or more occupied sites.

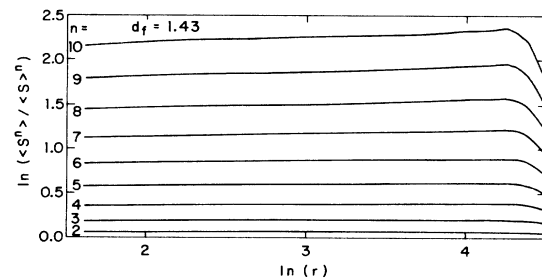


FIG. 6. Dependence of $\ln(\langle S^n \rangle / \langle S \rangle^n)$ on $\ln(r)$ for the 2D cluster-cluster aggregates for $n = 2-10$. For positive n these moments are essentially independent of r (the radius measured from an occupied particle).

$$P'_s(l) \sim S^{-2} f'(S/l^{d_f}). \quad (6)$$

Although this scaling form is different from that given in Eq. (2), no new parameters are introduced. The scaling form given in Eq. (6) can be understood in terms of that given in Eq. (2) since each of the S particles in a region of size l is also at the center of a region of the same size containing approximately S particles (i.e., $P_s \approx SP'_s$). The moments $\langle S^n \rangle / \langle S \rangle^n$ were also measured for the distribution of mass within the grid elements of area $l \times l$. The dependence of these moments on l is shown in Fig. 5(b). The quantities $\langle S^n \rangle / \langle S \rangle^n$ have very little dependence on l or r for both the screened-growth clusters and the cluster-cluster aggregates. At large distances $\langle S^n \rangle / \langle S \rangle^n$ decreases rapidly with decreasing l or r but this is a result of the fact that we only recorded the mass within each area for masses up to 2500 particles or occupied lattice sites. For very large values of r or l some areas contain more than 2500 sites or particles and omission of these areas artificially narrows the distribution.

We have also measured some of the negative moments. Figure 5(c) shows the dependence of $\langle S^n \rangle / \langle S \rangle^n$ for n lying in the range $-1 \geq n \geq -10$. The results shown in Fig. 5(c) are for screened-growth clusters with a fractal dimensionality of 1.5; similar results were obtained for $d_f = 1.25$ and 1.75. The quantities $\langle S^n \rangle / \langle S \rangle^n$ were also determined as a function of r for areas centered on randomly selected occupied sites. In this case these moments are, in contrast to the results shown in Fig. 5(c), essentially independent of r . The reason for this contrasting behavior is that some of the grid elements of size l contain only a few occupied lattice sites and it is these elements which dominate $\langle S^n \rangle$ for negative n . For large negative values of n , $\langle S^n \rangle$ will be dominated only by those grid areas containing one occupied site. For areas centered on occupied sites the minimum mass scales as r^{d_f} .

If the areas are centered either on random positions in space or on randomly occupied sites, we expect that $\langle S \rangle$ will be proportional to X^{d_f} , where X is the size of the areas. Figure 7(a) shows the dependence of $\langle S \rangle$ on r for areas centered on occupied sites and Fig. 7(b) shows the dependence of $\langle S \rangle$ on l for areas centered on random positions for screened-growth clusters with fractal dimensions of 1.25, 1.5, and 1.75. These results are consistent with the idea that $\langle S \rangle \sim r^{d_f}$ and l^{d_f} , but the dependence of $\ln \langle S \rangle$ on $\ln(l)$ in Fig. 7(b) is not particularly linear. These deviations from linearity may be a result of both finite-size effects and cluster-to-cluster fluctuations. These effects could be reduced by generating larger numbers of larger clusters but this would require very large amounts of computer time. For the grid areas of length l the dependence of the number of occupied areas on l has also been measured [Fig. 7(c)]. The results shown in this figure are consistent with the idea that $N(l) \sim l^{-d_f}$, where $N(l)$ is the number of occupied areas of size l .

Since single occupied areas play an important role in the negative moments ($\langle S^n \rangle / \langle S \rangle^n$ for $n < 0$), the num-

ber of areas of length l containing just one occupied lattice site, $N_1(l)$, has also been measured [Fig. 7(d)]. Our results indicate that $N_1(l) \sim l^{-\sigma}$, where the exponent σ has an effective value of about 2.39, 2.80, and 3.60, respectively, for $d_f = 1.25, 1.5,$ and 1.75 . Since the number of occupied regions of size l [$N(l)$] scales with increas-

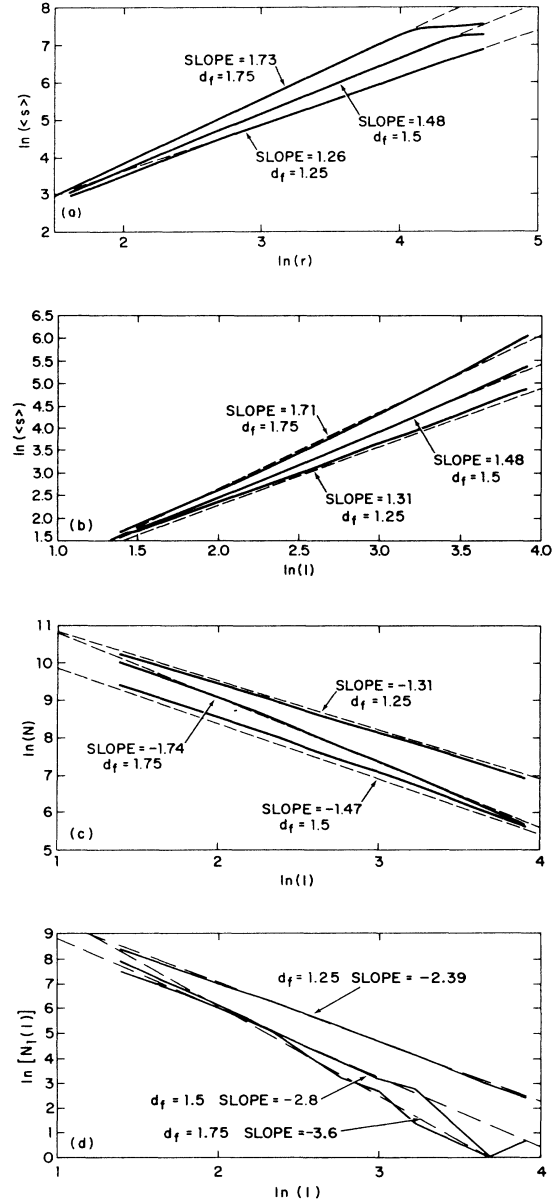


FIG. 7. (a) and (b) show the dependence of $\langle S \rangle$ on r and l for screened-growth clusters with fractal dimensions of 1.25, 1.50, and 1.75. $\langle S \rangle$ is obtained by averaging the occupancy over all areas of size r and over all occupied areas of size l (lattice units). Here r is the distance measured from a randomly selected occupied site and l is the grid size in a grid which covers a 400×400 site block at the center of each cluster. (c) shows the dependence of the number of occupied grid elements on l and (d) shows the dependence of the number of singly occupied grid elements on l .

ing l according to $N(l) \sim l^{-d_f}$, then $\langle S^n \rangle \rightarrow l^{d_f - \sigma}$ and we expect that $-(1/n)[\ln(\langle S^n \rangle / \langle S \rangle^n)]$ should have a linear dependence on $\ln(l)$ with a slope δn given by $\delta n = d_f - (1/n)(d_f - \sigma)$. Indeed, these predicted slopes are in good agreement with the slopes obtained from the results shown in Fig. 8. For example, we find that δ_{10} has values about 1.52, 1.33, and 1.23, respectively, for $d_f = 1.75, 1.50,$ and 1.25 . The results shown in Figs. 5(c) and 8 suggest that only two exponents (d_f and σ) may be needed to describe the scaling properties of the negative mass moments. This is illustrated in Fig. 8(b) where we show the dependence of $\tau(n)$ on n for the screened-growth clusters. Here $\tau(n)$ is defined by

$$Z_n \sim l^{-\tau(n)}, \quad (7)$$

where $Z(n)$ is $\langle S^n \rangle / \langle S \rangle^n$. The exponents $\tau(n)$ were obtained for 80 different values of n in the range $-10 \leq n \leq 10$ [in general, n is not an integer and the dependence of $\tau(n)$ on n for $-10 \leq n \leq 2$ is shown in Fig. 8(b)]. Figure 8(b) is consistent with the idea that the dependence of $\tau(n)$ on n can be divided into two regions corresponding to the positive and negative moments. For n positive $\tau(n) \approx 0$ and for the negative moments $\tau(n)$ decreases linearly with decreasing n . We expect that the slopes of the curves shown in Fig. 8(b) should have a value of $\sigma - d_f$. The measured slopes are 1.22, 1.38, and 1.68, respectively, for screened-growth clusters with fractal dimensions (D) of 1.25, 1.5, and 1.75, respectively. The corresponding values of $\sigma - d_f$ obtained from Fig. 7(d) are 1.16, 1.30, and 1.85, respectively. The quantitative agreement is reasonably good and these re-

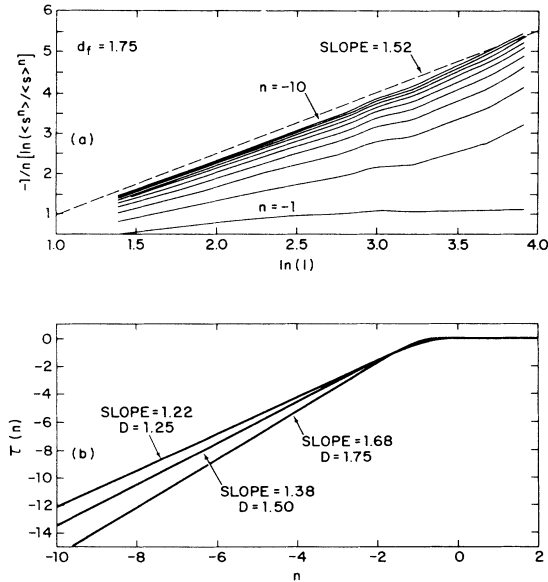


FIG. 8. (a) shows the dependence of the moments $\langle S^n \rangle / \langle S \rangle^n$ for screened-growth clusters with a fractal dimension of 1.75. Results for $-1 \geq n \geq -10$ are shown. (b) shows how the exponent $\tau(n)$ [obtained from results similar to those shown in (a)] depend on n for both integer and noninteger values of n in the range $-10 \leq n \leq 2$.

sults do support the qualitative picture suggested above. For mass distributions in areas of size r measured from an occupied site we expect that the minimum value of S will scale with r according to $S_{\min} \sim r^{d_f}$ (except for extremely rare events) so that $\delta_n \rightarrow 0$ for $n \rightarrow \infty$ in accord with our simulation results.

A similar numerical study has been applied to off-lattice DLA (Ref. 27) clusters. Thirty-seven 50 000 particle clusters were generated using algorithms described previously.²⁸ The quantities $N_s(r)$ were obtained for $r = 2-20$ diameters in steps of one diameter. In Fig. 9(a) we plot $\ln N_s(r)$ versus $\ln S$. In this figure we already see deviations from Eq. (2). Instead of a slope of -1 predicted by Eq. (2) we obtain a slope of -0.89 . Also, we could not fit our data to the scaling form Eq. (2) and the

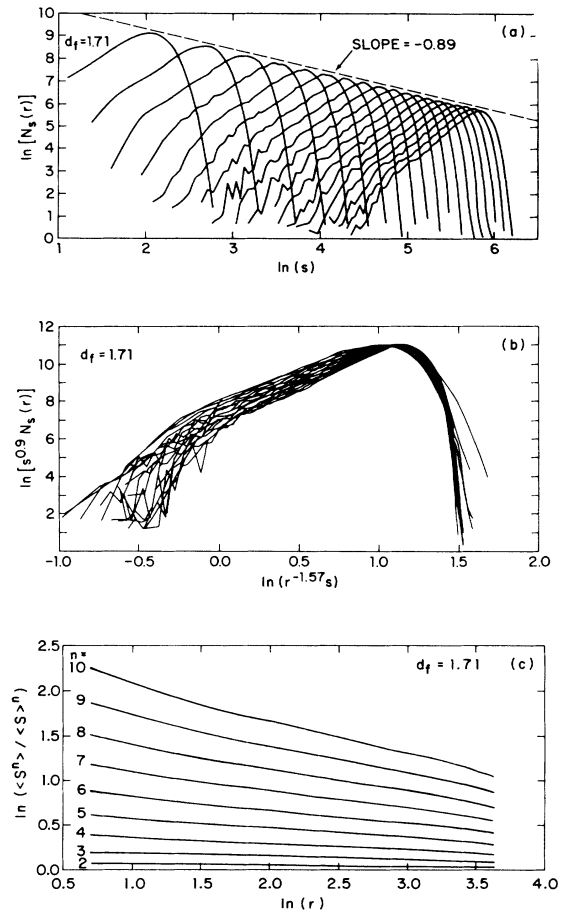


FIG. 9. The mass distribution N_s for 2D off-lattice DLA clusters is shown in (a). Each curve corresponds to a different value of the distance (r) (1–20 diameters in steps of one diameter). (b) shows the results of an attempt to scale these curves using the scaling form [Eq. (2)] which succeeded for the screened-growth clusters and cluster-cluster aggregates. The failure of this scaling procedure indicates that off-lattice DLA is not a self-similar fractal. (c) shows the dependence of $\langle S^n \rangle / \langle S \rangle^n$ on r (the distance from a randomly selected particle).

“best” scaling fit to Eq. (2), which is not good when compared to the earlier scaling results, is shown in Fig. 7(b). This best scaling was achieved assuming the formula $N_s(r) \sim S^{-0.9} f(S/r^{1.57})$. This form cannot be correct for two reasons: (i) it cannot be normalized, and (ii) it predicts $\langle S^n \rangle / \langle S \rangle^n \sim r^{-0.157n + 0.157}$, in disagreement with the numerical data shown in Fig. 9(c). In Fig. 9(c) we plotted $\ln(\langle S^n \rangle / \langle S \rangle^n)$ versus $\ln(r)$. Here the negative slope has much smaller values than those predicted in (ii), although the log-log plots shown in Fig.

7(c) look reasonably linear and suggest an infinite family of exponents. Power-law behavior with negative exponents cannot be the asymptotic form since $\langle S^n \rangle / \langle S \rangle^n$ has a minimum value of 1.0. These results indicate that DLA has a more complex internal structure than cluster-cluster aggregates or screened-growth clusters. Other recent simulations^{29–31} have led to similar conclusions. The decrease of $\langle S^n \rangle / \langle S \rangle^n$ with increasing r suggests that the DLA structure is more uniform on larger length scales than at shorter distances.

-
- ¹Kinetics of Aggregation and Gelation, edited by F. Family and D. P. Landau (Elsevier–North-Holland, Amsterdam, 1984).
- ²On Growth and Form: Fractal and Nonfractal Patterns in Physics, NATO Advanced Study Institute, Series E100, edited by H. E. Stanley and N. Ostrowsky (Martinus Nijhoff, Dordrecht, 1983).
- ³Fractals in Physics, Proceedings of Sixth Trieste International Symposium on Fractals in Physics, edited by L. Pietronero and E. Tosatti (North-Holland, Amsterdam, 1986).
- ⁴R. Jullien, R. Botet, and M. Kolb, *La Recherche* **16**, 1334 (1985).
- ⁵H. J. Herrmann, *Phys. Rep.* **136**, 154 (1986).
- ⁶T. A. Witten and M. E. Cates, *Science* **232**, 1607 (1986).
- ⁷L. M. Sander, *Sci. Am.* **256**, 94 (1986); *Nature* **322**, 789 (1986).
- ⁸B. B. Mandelbrot, *The Fractal Geometry of Nature* (Freeman, New York, 1982).
- ⁹P. Meakin, A. Coniglio, H. E. Stanley, and T. A. Witten, *Phys. Rev. A* **34**, 3325 (1986).
- ¹⁰T. C. Halsey, P. Meakin, and I. Procaccia, *Phys. Rev. Lett.* **56**, 854 (1986).
- ¹¹B. B. Mandelbrot, *J. Fluid Mech.* **62**, 331 (1974).
- ¹²H. G. E. Hentschel and I. Procaccia, *Physica D* **8**, 835 (1983).
- ¹³L. de Archangelis, S. Redner, and A. Coniglio, *Phys. Rev. B* **31**, 4725 (1985).
- ¹⁴A. Renyi, *Probability Theory* (North-Holland, Amsterdam, 1970).
- ¹⁵R. Benzi, G. Paladin, G. Parisi, and A. Vulpiani, *J. Phys. A* **17**, 3521 (1984).
- ¹⁶T. C. Halsey, M. H. Jensen, L. P. Kadanoff, I. Procaccia, and B. I. Shraiman, *Phys. Rev. A* **33**, 1141 (1986).
- ¹⁷U. Frisch and G. Parisi, in *Turbulence and Predictability in Geophysical and Fluid Dynamics*, edited by M. Ghil, R. Benzi, and G. Parisi (North-Holland, Amsterdam, 1985).
- ¹⁸H. E. Roman, A. Bunde, and S. Havlin (unpublished).
- ¹⁹P. A. Rikvold, *Phys. Rev. A* **26**, 674 (1982).
- ²⁰P. Meakin, *Phys. Rev. B* **28**, 6718 (1983).
- ²¹P. Meakin, F. Leyvraz, and H. E. Stanley, *Phys. Rev. A* **31**, 1195 (1985).
- ²²L. M. Sander, in *Kinetics of Aggregation and Gelation*, edited by F. Family and D. P. Landau (Elsevier–North-Holland, Amsterdam, 1984), p. 13.
- ²³P. Meakin, *Phys. Rev. Lett.* **51**, 1119 (1983).
- ²⁴M. Kolb, R. Botet, and R. Jullien, *Phys. Rev. Lett.* **51**, 1123 (1983).
- ²⁵R. Botet, R. Jullien, and M. Kolb, *J. Phys. A* **17**, L75 (1984).
- ²⁶P. Meakin, *Phys. Lett.* **107 A**, 269 (1985).
- ²⁷T. A. Witten and L. M. Sander, *Phys. Rev. Lett.* **47**, 1400 (1981).
- ²⁸P. Meakin, *J. Phys. A* **18**, L661 (1985).
- ²⁹T. C. Halsey and P. Meakin, *Phys. Rev. A* **32**, 2546 (1985).
- ³⁰P. Meakin and T. Vicsek, *Phys. Rev. A* **32**, 1026 (1985).
- ³¹M. Kolb, *J. Phys. (Paris) Lett.* **46**, L67 (1985).